Environment Effects on the CO Vibrational Shifts in Erbium Complexes: A Quantum Chemical Study

Massimo Ottonelli,* Gianfranco Musso, and Giovanna Dellepiane

Università di Genova, Dipartimento di Chimica e Chimica Industriale, Via Dodecaneso 31, I-16146 Genova, Italy

Received: August 12, 2008; Revised Manuscript Received: September 30, 2008

The stability of lanthanide complexes and the efficiency of the energy transfer process, which makes these molecules interesting materials for technological applications, are correlated to the chemical environment surrounding the metal ion. In particular the efficiency depends on the relative position of the antenna (the ligand moiety that acts as photon absorption center) and the lanthanide ion (the emitting center), while the stability of the complex is correlated to the strength of the coordination between the rare earth and the ligands. For these reasons, knowledge of the structural properties of the complex is an interesting task to achieve. Since a large number of ligand structures hold the carboxylate group (COO^-), which is used as an anchor for binding the antennae to the lanthanide ion, in this work we will show how the vibrational shifts of this group, induced by the interactions between the carboxylate moiety and the metal center of the lanthanide complex, can be used for obtaining in a simple way information on the structure of the chemical environment surrounding the lanthanide ion.

1. Introduction

Lanthanide complexes have raised increasing interest for their potential applications in several research areas such as in the biomedical field, where use of these complexes as chemosensors for in vivo applications has been recently described,[1] and in the technological field, where the design of efficient light-emitting devices and their use in optical technology has been reported in several papers.[2,3]

The physicochemical property of lanthanide complexes that is the basis for developing efficient light-conversion molecular devices is the luminescence intensity. This effect originates from the intramolecular energy transfer from one excited ligand to the *f*-electronic structure of the metal ion, and is critically dependent on the molecular geometry of the ligands aggregate as well as on the chemical nature of the single aggregate unit. In particular, the ligand should be able to promote the energy transfer of the optical excitation and, through suitable functional groups, to efficiently saturate the lanthanide coordination sphere and make a strong binding interaction with the rare earth ion. The saturation of the sphere should minimize the quenching of the complex luminescence that may occur due to the interactions with the solvent, while a strong binding should increase the complex stability. In turn, an increased complex stability implies an increased processability of the material, an important factor for its technological applications. One suitable functional group to this end is the carboxylate moiety that is present in several ligand structures. Moreover, due to the increasing interest in the molecular design of hetero- or homometallic multinuclear complexes (which are promising materials for practical applications due to their photophysical and magnetic properties[4]) the control of the metal−ligand coordination type represents an important task to achieve. Ligands designed with different carboxylate clamps can be fully coordinated to the same metal ion or, due to the presence of competitive ligands and of steric hindrance, only one COO^- group of the clamp at a time may be bonded to the metal center. In the latter case the rest of the carboxylate moieties remain free to coordinate to other metal ions of the same or of a different chemical nature.

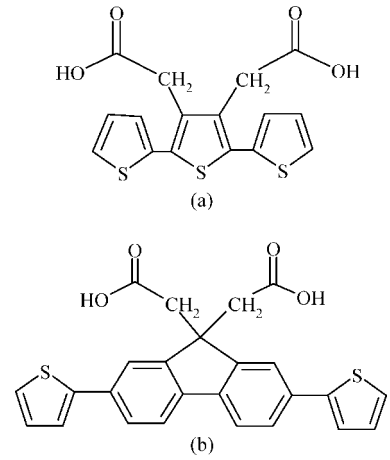

Figure 1. Scheme of molecular structures of $L1H_2$ (a) and $L2H_2$ (b).

The aim of this work is to study quantum chemically the vibrational shifts induced by the interactions between the carboxylate moiety and the metal center of lanthanide complexes, and to show how they can be used for obtaining in a simple way information on the structure of the chemical environment surrounding the lanthanide ion. A similar approach has been used for the carbonyl group in molecular systems of biological interest.[5] We use as representative systems Er^{3+} complexes prepared with a new class of oligothiophene and thiophenefluorene ligands, {4′-(hydroxycarbonyl)methyl-[2,2′;5′,2″]terthiophen-3′-yl}acetic acid and 9-(hydroxylcarbonyl)-methyl-2,7-dithien-2-yl[fluoren-9-yl]acetic acid, which we denote as $L1H_2$ and $L2H_2$, respectively, see Figure 1. Details of their synthesis and optical properties have been reported in a

* To whom correspondence should be addressed. Phone: +39-010-353-6090. Fax: +39-010-353-6199. E-mail: massimo@chimica.unige.it.

10.1021/jp807203n CCC: $40.75
Published on Web 10/29/2008

previous work.[6] We recall that IR spectra of the complexes show significant differences in the carboxylate vibrational frequency region in relation to the presence of phenanthroline or pyridine as a competitive ancillary ligand.

To be specific, in this paper we will show that the variations of the vibrational frequencies associated with the normal modes of the carboxylate groups [i.e., the symmetric (*s*) and asymmetric (*a*) CO stretchings] with respect to those of the isolated COO^-, as well as of their mutual difference, can be correlated to the topology of the carboxylate−metal ion binding mode, and to the distance between the carboxylate moiety and the metal ion. More generally, this implies that in the presence of the COO^- moiety as a coordinated group useful information on the structure of the lanthanide complex can be obtained in a simple way from its IR spectra. This analysis could be of particular importance for cases where single crystals of the complex, suitable for X-ray characterization, cannot be obtained. Finally, through a correlation between the vibrational shift of the carboxylate group and the lanthanide−antennae separation (*R*), an estimate of the value of *R* can be obtained that can give information on the efficiency of the energy transfer process in the luminescence of the complex.

2. Results and Discussion

Due to their large size, the L1 and L2 erbium complexes are modeled by replacing the coordination compounds with the ligands salts. Although this choice may appear too severe an approximation, it will be shown to be adequate for reproducing well the IR spectra of the complexes, at least in the frequency region of the carboxylate stretching vibrational modes. In this respect it is of special interest to request a simple and efficient modeling of the different sterical hindrances and coordination abilities of the phenanthroline and pyridine ancillary ligands. Unlike pyridine, phenanthroline has in fact a large steric hindrance and two coordination sites (the nitrogen atoms), which implies that in the presence of the latter/former ancillary ligand the coordination sphere of the lanthanide will be accessible to only one/all two COO^- moieties of the actual ligand. Here this request will be simply answered through a proper choice of the salt counterion. As we shall see, use of a univalent ion such as Na^+ will be able to model the case of a packed coordination sphere of the rare earth ion where only *a single* carboxylate moiety can be bound (bidentate coordination, see below), while with a divalent ion such as Zn^{2+} the case can be modeled in which *both* COO^- groups can be accessed by the rare earth ion (monodentate coordination). This way of modeling lanthanide complexes is the basis of our pseudocoordination center method, which has been proposed and discussed elsewhere.[7−9] This semiempirical approach appears to be an ideal compromise to predict with an acceptable computational cost the structure of the whole real lanthanide complex (that usually contains large ligands), while ab initio calculations are usually performed on a complex containing small to medium ligands, or on isolated ligands themselves.[10−13]

2.1. Optimized Geometries. The ground state geometries of the $L1Na_2$, L1Zn, $L2Na_2$, and L2Zn model systems, as well as those of the $L1H_2$ and $L2H_2$ acids and their isolated dianions ($L1^{2-}$ and $L2^{2-}$), have been optimized in the framework of the DFT B3LYP/6-31G(d) approach[14] with no use of any symmetry constraint. For the L1 salts two minima are found, corresponding to the *syn* and *anti* conformations of the two carboxylate groups with respect to the molecular plane of the central thiophenyl ring. The *syn* arrangement results in the most stable geometry throughout, by an amount of 20.7 kcal/mol for $L1Na_2$ and of 0.83 kcal/mol for L1Zn, respectively. In the following we will show the importance of taking into consideration the presence of two such minima for modeling IR spectra of the erbium complexes. The details of all optimized geometries are given in Figures 1s−5s of the Supporting Information. Note that all of the resulting geometries show an almost exact C_2 symmetry.

Deprotonation can be seen to only slightly affect the molecular structure of the two ligands, notable geometry variations (around 0.08 Å) being found only in methylcarboxylate groups. A similar effect occurs in the salts where, however, the important point is that the highest bond length variation is strictly correlated to the nature of the counterion. For the univalent counterion (Na^+) a *bidentate* coordination of the COO^- moiety is obtained, which almost removes any CO bond length difference, especially for the *anti* conformation (see Figure 1s, Supporting Information). On the contrary, the divalent counterion (Zn^{2+}) is able to interact with both carboxylate groups, implying the coordination results of a *monodentate* type, and the CO bonds within each carboxyl moiety become definitely unequivalent.

2.2. Simulated IR Spectra. The different geometries of the carboxylate moiety imply different IR signatures. In fact, as pointed out in the literature for monocarboxylated salts,[15−18] the frequency shifts of the *s* [$\nu_s(COO^-)$] and *a* [$\nu_{as}(COO^-)$] stretching modes with respect to those of the free carboxylate anion are a function of the metal ion−carboxylate coordination. In the case of a monodentate chelation, the two CO bonds in the COO^- moiety have a double- and a single-bond character, respectively. This implies that the $\nu_{as}(COO^-)$ normal mode increases in frequency (becoming closer to a C═O stretching), and conversely the frequency of the $\nu_s(COO^-)$ stretching decreases (becoming closer to a C−O stretching). On the other hand, for a bidentate coordination the CO bond order variations should be in the same sense, and the same is expected to be true for the frequency shifts of the two stretching modes. Moreover, as the CO bond lengths result in our case to be slightly increased with respect to those of the isolated $-COO^-$ group (see Figure 2s(a), Supporting Information), both shifts are expected to be negative. To be specific, for monocarboxylated salts the $\nu_s(COO^-)$ and $\nu_{as}(COO^-)$ normal modes show strong absorption bands in the ranges 1406−1414 and 1530−1545 cm^{-1}, respectively,[15−18] the frequency difference between the two bands being generally greater than 140 cm^{-1} for a monodentate and around 100 cm^{-1} for a bidentate chelation.[15]

In our cases we have two carboxylate groups in each ligand, and a total of four COO^- stretching modes [$\nu_s^+(COO^-)$, $\nu_s^-(COO^-)$, $\nu_{as}^+(COO^-)$, and $\nu_{as}^-(COO^-)$]. A sketch of these normal modes can be found in Figure 6s (Supporting Information) together with the corresponding ones for the COOH group and for the $(COOH)_2$ H-bond dimer. This mixing of the COO^- normal modes implies that in the IR spectra (i) the vibrational frequency ranges of the *a* (*s*) stretching are increased (decreased) with respect to those of the singly carboxylated units and (ii) the intensity associated to a particular normal mode becomes highly dependent on the reciprocal orientation and weight of the two constituent local modes in the linear combination. Point (ii) may have notable consequences in selected cases. For instance, for the *syn* conformation the $\nu_s^+(COO^-)$ and $\nu_{as}^+(COO^-)$ normal modes are those with enhanced absorption intensity, while the intensity of the $\nu_s^-(COO^-)$ and $\nu_{as}^-(COO^-)$ modes is much lower or even zero, but the opposite is true for the *anti* conformation. Both types of chelation increase the difference in frequency between the *a* and *s* modes with respect to the

TABLE 1: Experimental and Calculated Main Absorption Bands in the 1300−1750 cm^{-1} IR Spectra Region for the L1 and L2 Compounds

molecule	exptl[a]	model system	calcd freq[f]
		L1	
$L1H_2$	1696 s	$L1H_2$	1708 [ν_d^-(COOH), 358]
	1641 w	(dimer)	1661 [ν_d^+(COOH), 7]
	1422 m		1412 [$\delta_{\parallel}$(H-bond),159]
$L1Na_2$[b]	1642 s	$L1Na_2$	1622 [ν_{as}^+(COO$^-$), 949]
	1578 s	(*syn*)	1593 [ν_{as}^-(COO$^-$), 53]
	1461 m		1440 [methylene bending, 18]
	1383 s		1362 [ν_s^+(COO$^-$), 271]
	1361 m		1340 [methylene + ring bending mode, 40]
	1319 m		1323 [ν_s^-(COO$^-$), 127]
L1C1[c]	1740 s	L1Zn	1743 [ν_{as}^-(COO$^-$), 474]
	1465 s	(*anti*)	−
	1373 m		−
	1241 s		1212 [ν_s^+(COO$^-$)+ methylene twisting, 294]
L1C2[b]	1577 s	$L1Na_2$	1548 [ν_{as}^-(COO$^-$), 535]
	1529 m[e]	(*anti*)	1531 [ν_{as}^+(COO$^-$) + ring bending, 156]
	1401 s		1367 [ν_s^-(COO$^-$), 307]
		L2	
$L2H_2$	1709 s	$L2H_2$	1757 [ν_{anti}^-(COOH), 407]
	1604 w		1595 [central ring bending, 12]
	1470 m		1462 [central ring bending, 86]
	1420 m		1403 [central + thiophene rings bending, 40]
L2C2[d]	1557 s	$L2Na_2$	1550 [ν_{as}^-(COO$^-$), 625]
	1469 m		1446 [methylene bending, 40]
	1425 s		1405 [methylene + ring ben-ding mode, 123]
	1396 s		1397 [ν_s^-(COO$^-$), 226]

[a] The values of the vibrational frequencies are taken from ref 5. Strong (s), medium (m), and weak (w) absorption band. [b] Experimental data obtained from Destri et al., see ref 5. [c] L1 erbium complex with pyridine as coligand, see ref 5. [d] L1 or L2 erbium complex with phenanthroline as coligand, see ref 5. [e] Shoulder of the band at 1577 cm^{-1}. [f] Gaussian package,[9] B3LYP/6-31G* model, scaling factor 0.96.[14] In brackets the vibrational assignment (main components of the normal mode, see Figure 6s, Supporting Information) and the calculated IR intensity (KM/mol) are shown.

case of a single COO$^-$ group, and both the *in-phase* and *out-of-phase* combinations can become experimentally observable.

In Table 1 the experimental and computed [B3LYP/6-31G(d), scaling factor 0.96, see ref 19] frequency peak positions are given for the main absorption bands in the 1300−1750 cm^{-1} region of the IR spectrum for all systems of interest [L1C1 (the erbium complex with L1 and pyridine), L1C2 and L2C2 (the erbium complexes with L1 or L2 and phenanthroline)] and their theoretical models adopted here. A satisfactory agreement between the two sets of results is seen to have been obtained. In both $L1H_2$ and $L2H_2$ acids H-bond formation must be expected, and it would be desirable to model such systems with a dimer form. This, however, has been done for acid $L1H_2$ only, due to the high computational times that would have been required to do the same for the $L2H_2$ dimer geometry optimization and subsequent force calculation. The theoretical IR spectrum of the $L1H_2$ dimer predicts an absorption band at 1708 cm^{-1} with an intensity in very good agreement with the strong absorption band observed at 1696 cm^{-1}, while a corresponding calculation on the isolated $L1H_2$ molecules gives a result that is in error by 69 cm^{-1}. Good results are also obtained for the other two bands of the dimer, which are predicted at 1661 and 1412 cm^{-1}, with errors of 20 and −10 cm^{-1}, respectively. We remark that the simulated spectrum of $L1H_2$ well reproduces also the out-of-plane H-bond bending mode, $\delta_{\perp}$(H-bond), typical of the acid dimeric form (at 935 cm^{-1} vs an experimental value of 914 cm^{-1}).

For $L2H_2$, the fact that the highest COOH experimental frequency falls 13 cm^{-1} higher than the corresponding band of $L1H_2$ suggests the dimer is weakly bound, as also shown by the fact that the isolated-molecule simulated spectrum is in nice agreement with the experimental data in this spectral region.[20] Only the 48 cm^{-1} error in the highest COOH frequency can be attributed to the neglect of dimer effects.

The effect of the rare earth ion−carboxylate coordination on the vibrational frequencies associated to the carboxylate moieties is analyzed starting from the experimental data for L1C2 and L2C2 complexes. First of all, from the data of Table 1 it emerges that the experimental results for the L1C2 complex and the $L1Na_2$ salt are remarkably different, an effect that our model should be able to justify. In this respect we recall that geometry optimization on $L1Na_2$ had predicted two minimum structures, namely a more stable *syn* one, where the two COO$^-$ moieties point in the same direction, and an *anti* one 20.7 kcal/mol higher, where the two COO$^-$ moieties do the opposite. It appears most reasonable to suppose that the former should model the $L1Na_2$ salt, while the difference in the L1C2 and $L1Na_2$ experimental spectra suggests that the latter conformation could be a model of L1C2. In fact, despite the higher energy of this form in the isolated salt, during the actual complexation its geometry can be believed as more suitable for docking in the crowded coordination sphere of the rare earth ion. Comparison of the experimental and quantum chemical IR frequencies confirms the above hypotheses. In the L1C2 spectrum two strong absorption bands are observed at 1577 and 1401 cm^{-1} that are satisfactorily reproduced from the force calculations, with errors of −29 and −34 cm^{-1}, respectively. The theoretical analysis allows the assignment of these absorption bands to the ν_{as}^-(COO$^-$) (peak at 1577 cm^{-1}) and ν_s^-(COO$^-$) (peak at 1401 cm^{-1}) normal modes. An error of only 2 cm^{-1} is found for the medium absorption band observed at 1529 cm^{-1},[21] and due to a normal mode that can be mainly described as the asymmetric in-phase COO$^-$ stretching ν_{as}^+(COO$^-$). The experimental spectrum of the $L1Na_2$ salt exhibits a larger number of signatures in the frequency range considered here. In particular, three strong bands are present, at 1642, 1578, and 1383 cm^{-1}, due to the ν_{as}^+(COO$^-$), ν_{as}^-(COO$^-$), and ν_s^+(COO$^-$) normal modes, respectively. Of the three medium bands at 1461, 1361, and 1319 cm^{-1}, the two higher energy ones are assigned to methylene bendings and the third one to the ν_s^-(COO$^-$) normal mode. The theoretical errors in the frequency are less than or equal to 21 cm^{-1}.

It can be seen that in these systems the frequency of the *a* (*s*) carboxylate normal mode is increased (decreased) with respect to the single COO$^-$ case, due to the vibrational interaction between the two groups. Consequently, for the chelating bidentate coordination, the difference in frequency between the *a* and *s* COO$^-$ stretching [$\Delta\nu = \nu_{as}^-$(COO$^-$) − ν_s^-(COO$^-$)], which typically lies around 100 cm^{-1} for the soaps,[15] appears to be enhanced here, its values being $\Delta\nu$ = 176 cm^{-1} for L1C2 and $\Delta\nu$ = 259 cm^{-1} for $L1Na_2$. The difference between the latter values can be explained by the facts that in the $L1Na_2$ *anti* structure (modeling L1C2) the bidentate coordination results in a symmetrical arrangement (equal CO bond lengths), while in *syn* $L1Na_2$ an appreciable difference in the CO bond lengths is found (asymmetrical

bidentate coordination). The interested reader is referred to Figure 2s in the Supporting Information. This asymmetry implies different CO bond orders, which is sufficient for some increase (decrease) of the frequency associated to the *a* (*s*) COO^- normal mode, which in turn leads to an increased $\Delta\nu$. As an example (see Table 1), for $L1Na_2$ the $\nu_{as}^+(COO^-)$ normal mode falls at 1642 cm^{-1}, while for L1C2 the corresponding $\nu_{as}^-(COO^-)$ mode falls at 1577 cm^{-1}. As a final comment, our model systems nicely reproduce the main absorption bands of the experimental spectra in the 1300−1750 cm^{-1} region in energy and in intensity, with the exception of the relative intensities of the $\nu_s^+(COO^-)$ and $\nu_{as}^-(COO^-)$ bands of the $L1Na_2$ salt (see Table 1). While quantum chemically computed IR intensities can always be affected by some error, the wrong predicted intensity ratio between the two bands in this case can probably be explained in terms of effects of the type referred to in point (ii) in the second paragraph of Section 2.2. In this respect the theoretical modeling could be improved by taking into account the effect of somewhat different conformations of the sodium carboxylate moiety.[22]

A similarly satisfactory agreement between the theoretical modeling and experimental results is found for the L2C2 case. The force calculations reproduce the observed bands at 1557, 1469, 1425, and 1396 cm^{-1} with errors of −7, −23, −20, and 1 cm^{-1}, respectively. The $\nu_{as}^-(COO^-)$ mode is assigned to the band at 1557 cm^{-1} and $\nu_s^-(COO^-)$ to the band at 1396 cm^{-1}, and a value of 161 cm^{-1} is obtained for $\Delta\nu$. This result agrees with that obtained for the L1C2 complex, in that a symmetric bidentate chelation of two carboxylate groups is found in this case too, as could be seen in Figure 3s(a) (Supporting Information). Besides the frequency separation, also the absolute positions of the peaks of the two modes are comparable with the L1C2 results. On this basis, we can extrapolate that for molecular systems with two ancillary COO^- groups, in the case of a symmetric bidentate chelation, the $\nu_{as}^-(COO^-)$ mode can be expected to fall in the range 1550−1580 cm^{-1} and the $\nu_s^-(COO^-)$ in the range 1390−1405 cm^{-1}. As a final comment, the discrepancy between the theoretical and experimental IR intensities of the bands at 1405 and 1425 cm^{-1}, respectively, can probably be explained by the presence in this zone of the phenanthroline intense peak at 1422 cm^{-1},[23] overlapping those of the L2 ligands.

For the erbium complex prepared in the presence of pyridine, only experimental data for the L1C1 complex are available. With respect to L1C2, where the competitive ligand was phenanthroline, the steric hindrance due to the pyridine should not hamper the coordination of both the carboxylate groups by the rare earth ion. In fact, since the number of oxygen atoms surrounding the metal coordination sphere is increased, and not all of the available oxygen sites are required to saturate the sphere itself, and the strength of the metal−oxygen bond is proportional to the amount of negative charge on the oxygen atom, we should expect the monodentate coordination of the carboxylate to be energetically favored. Geometry optimization on the L1Zn and L2Zn salts shows that the $Zn^{2+}-COO^-$ interaction is indeed of such a type [for a sketch see Figures 3s(b) and 5s(b), Supporting Information]. A further remark concerns the high asymmetry of the two CO bonds combined with the presence of an anchor point of large mass, which practically freezes the vibrational motion of the coordinated oxygen atoms, and makes the $\nu_{as}^-(COO^-)$ or the $\nu_{as}^+(COO^-)$ normal modes to be practically the out-of-phase or the in-phase linear combination of the double CO bond stretchings. We should accordingly expect the out-of-phase normal mode of the *anti* conformation to occur at a higher frequency with respect to the bidentate coordination or to the protonated form of the ligand.

For L1C1 a strong absorption band is detected at 1740 cm^{-1}, i.e. at a frequency definitely higher than those observed for L1C2 (1577 cm^{-1}), $L1Na_2$ (1642 cm^{-1}), or $L1H_2$ (1696 cm^{-1}). Since also for the L1Zn salt the geometry optimization gives an *anti* and a *syn* minimum structure, force calculations were done for both. The two resulting IR spectra are very similar; in Table 1 only the results for the L1Zn *anti* geometry are shown, because the *anti* IR frequencies reproduce somewhat better the experimental results, and moreover, as for L1C2, the L1C1 complex is expected to be best modeled by the *anti* form of L1Zn.

The band at 1740 cm^{-1}, assigned to the $\nu_{as}^-(COO^-)$ normal mode, is reproduced with an error of 3 cm^{-1}. The observed band at 1241 cm^{-1}, predicted with an error of −29 cm^{-1}, can be assigned to a normal mode that is mainly a combination of the $\nu_s^+(COO^-)$ stretching with a small amount of the methylene twisting. For the other two experimental bands at 1465 and 1373 cm^{-1} no correspondence with the computed spectrum is found. The first one could originate from the pyridine ligand, which has a strong band at 1450 cm^{-1}, while the band at 1373 cm^{-1} could be related to a L1Zn structure where one of the two carboxylate groups has a bidentate coordination, while the other one is monodentate. In fact, a force calculation performed on this geometry predicts an IR band at 1390 cm^{-1}, suggesting that in the L1C1 erbium complex both the coordination types could be present. The experimental frequency difference between the *a* and *s* COO^- stretchings, $\Delta\nu$, which for the monodentate coordination in the soaps exceeds 140 cm^{-1} and is usually around 150−160 cm^{-1},[15] for L1C1 increases to 499 cm^{-1}. Although no experimental spectrum for L2C1 is available for comparison, the $\nu_{as}^-(COO^-)$ and $\nu_s^+(COO^-)$ normal modes are predicted for L2Zn at 1755 and 1290 cm^{-1}, respectively. So also in this case the monodentate coordination gives a high value for $\Delta\nu = 465$ cm^{-1}, of an order of magnitude similar to that computed for L1C1 as modeled with L1Zn (531 cm^{-1}).

As a final point, we want to outline a side feature of our approach that can be of some interest. For the monodentate coordination (L1Zn and L2Zn model systems) a further improvement of the theoretical modeling can be achieved by examining the dependence of the spectrum on the metal ion−COO^- distance. In particular, for the spectrum range where the COO^- vibrational signatures fall (1300−1700 cm^{-1}), variation in the mutual distance between each carboxylate moiety and the metal ion is expected to cause corresponding changes in the frequency positions of the COO^- stretching modes. To assess the importance of such an effect, a series of force calculations have been performed for *syn* and *anti* L1Zn and for L2Zn, in which the Zn−O distance has been held fixed at different values, and the remaining geometry parameters have been fully optimized in each case. Figure 2 shows the dependence on the Zn−O distance of the frequency of the most intense normal mode [$\nu_{as}^-(COO^-)$ for L1Zn *anti* and L2Zn, and $\nu_{as}^+(COO^-)$ for L1Zn *syn*]. A monotonic linear dependence for *anti* L1Zn and L2Zn is observed, while *syn* L1Zn shows two distinct linear trends. The different behavior in the latter case can be explained in terms of a change in the clamping structure of the *syn* conformation for metal ion−COO^- distances around 1.9 Å, the metal ion lying "inside" or "outside" the clamp for distances lower or higher than this value. In the shift from the "inside" to the "outside" positions the two carboxylate groups are forced to open the clamp, which causes the asymmetry of the CO bonds to vary. Anyway, in all cases the slope of the

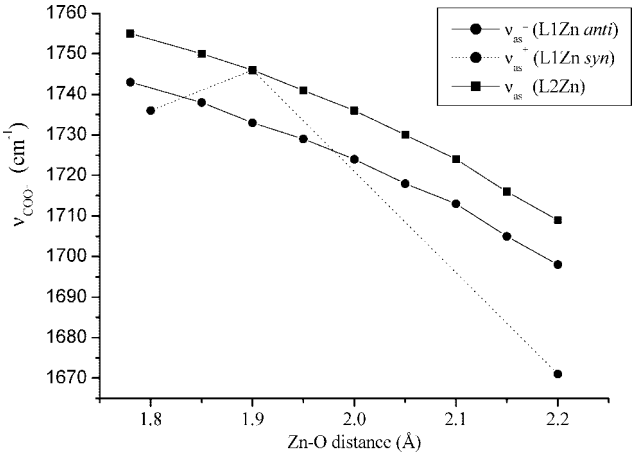

Figure 2. Plots of the calculated highest intensity vibrational frequencies of the COO^- group versus the Zn−O distance for the L1(L2)Zn salts.

linear dependence is sufficiently high to allow correlating an observed peak position with a corresponding metal ion (lanthanide)−COO^- estimated distance, a useful parameter for the evaluation of the energy transfer efficiency.

3. Conclusions

We have shown that the $\Delta\nu$ vibrational frequency shift of the carboxylate moiety in erbium complexes can be correlated with the chemical environments surrounding the rare earth ion. In this way information about the nature of the metal−COO^- coordination and distance can be achieved. In fact, for a dicarboxylate ligands like L1 or L2, a bidentate chelating coordination implies values of $\Delta\nu$ around 170 cm^{-1} (when symmetric) or 250 cm^{-1} (when asymmetric), while for a monodentate chelation this difference is further increased up to 500 cm^{-1}. The above separations between the asymmetric and symmetric COO^- stretchings are significantly different from each other, and sensibly higher with respect to the corresponding values for a soap. A similar behavior is found also for the absolute frequency of the highest energy normal mode, especially for a monodentate chelation. Specifically, for a symmetric bidentate chelation $\nu_{as}^{\pm}(COO^-)$ is expected to fall around 1550 cm^{-1}, and around 1750 cm^{-1} for a monodentate coordination.

Our modeling definitely allows us to attribute a monodentate chelating coordination to L1 (L2) complexes prepared in the presence of a bulky competitive ligand such as phenanthroline, and a bidentate one when the coordination sphere of the rare earth ion does not suffer significant steric hindrance.

Acknowledgment. The research was supported by the Italian MIUR through the RBNE033KMA and the PRIN 2007-2007PBWN44 projects.

Supporting Information Available: Additional figures giving bond lengths and dihedral angles between thiophenyl rings and some representative vibration modes for a molecular system with two interacting COO^- or COOH groups. This material is available free of charge via the Internet at http://pubs.acs.org.

References and Notes

(1) (a) Venturi, M.; Credi, A.; Balzani, V. *Molecular Devices and Machines-A Journey into the Nanoworld*; Wiley-VCH: Weinheim, Germany, 2003. (b) Special issue on fluorescent sensors: *J. Mater. Chem.* **2005**, *15*, 2617−2976.

(2) Wang, R.; Yang, J.; Zheng, Z.; Carducci, M. D.; Cayou, T.; Peyghambarian, N.; Jabbour, G. E. *J. Am. Chem. Soc.* **2001**, *123*, 6179.

(3) Bunzli, J. G.; Piguet, C. *Chem. Soc. Rev.* **2005**, *34*, 1048.

(4) Zibaseresht, R.; Hartshorn, R. M. *Aust. J. Chem.* **2005**, *58*, 345.

(5) Carey, P. R. *Chem. Rev.* **2006**, *106*, 3043.

(6) Destri, S.; Pasini, M.; Porzio, W.; Rizzo, F.; Dellepiane, G.; Ottonelli, M.; Musso, G. F.; Meinardi, F.; Veltri, L. *J. Lumin.* **2007**, *127*, 601.

(7) Ottonelli, M.; Izzo, G. M. M.; Musso, G. F.; Dellepiane, G.; Rizzo, F.; Tubino, R. *J. Phys. Chem. B* **2005**, *109*, 19249.

(8) Ottonelli, M.; Izzo, G. M. M.; Musso, G. F.; Dellepiane, G.; Tubino, R. *Opt. Mater.* **2006**, *28*, 714.

(9) Ottonelli, M.; Musso, G. F.; Rizzo, F.; Dellepiane, G.; Porzio, W.; Destri, S. *Mater. Sci. Eng., B* **2008**, *146*, 50.

(10) Ning, L.; Trioni, M. I.; Brivio, G. P. *J. Mater. Chem.* **2007**, *17*, 4464.

(11) Kim, H. J.; Lee, J. E.; Kim, Y. S.; Park, N. G. *Opt. Mater.* **2002**, *21*, 181.

(12) Gutierrez, F.; Rabbe, C.; Poteau, R.; Daudey, J. P. *J. Phys. Chem. A* **2005**, *109*, 4325.

(13) Aiga, F.; Iwanaga, H.; Amano, A. *J. Phys. Chem. A* **2007**, *111*, 12141.

(14) Frisch, M. J.; Trucks, G. W.; Schlegel, H. B.; Scuseria, G. E.; Robb, M. A.; Cheeseman, J. R.; Zakrzewski, V. G.; Montgomery, J. A., Jr.; Stratmann, R. E.; Burant, J. C.; Dapprich, S.; Millam, J. M.; Daniels, A. D.; Kudin, K. N.; Strain, M. C.; Farkas, O.; Tomasi, J.; Barone, V.; Cossi, M.; Cammi, R.; Mennucci, B.; Pomelli, C.; Adamo, C.; Clifford, S.; Ochterski, J.; Petersson, G. A.; Ayala, P. Y.; Cui, Q.; Morokuma, K.; Malick, D. K.; Rabuck, A. D.; Raghavachari, K.; Foresman, J. B.; Cioslowski, J.; Ortiz, J. V.; Baboul, A. G.; Stefanov, B. B.; Liu, G.; Liashenko, A.; Piskorz, P.; Komaromi, I.; Gomperts, R.; Martin, R. L.; Fox, D. J.; Keith, T.; Al-Laham, M. A.; Peng, C. Y.; Nanayakkara, A.; Gonzalez, C.; Challacombe, M.; Gill, P. M. W.; Johnson, B.; Chen, W.; Wong, M. W.; Andres, J. L.; Gonzalez, C.; Head-Gordon, M.; Replogle, E. S.; Pople, J. A. *Gaussian 98*, Revision A.7; Gaussian, Inc.: Pittsburgh, PA, 1998.

(15) Deacon, G. B.; Phillips, R. J. *Coord. Chem. Rev.* **1980)** , *33*, 227.

(16) Nakamoto, K. *Infrared spectra of Inorganic and Coordination Compounds*; Wiley: New York, 1986.

(17) Cotton, F. A. Wilkinson, G. *Advanced Inorganic Chemistry*; Wiley: New York, 1988.

(18) Marques, E. F.; Burrows, H. D.; da Graca Miguel, M. *J. Chem. Soc., Faraday Trans.* **1988**, *94*, 1729.

(19) Computational Chemistry Comparison and Benckmarks Database, http://cccbdb.nist.gov.

(20) The peak at 1420 cm^{-1} is rather sharp, although it is surrounded by a broad and structured band in the region 1410−1430 cm^{-1}, and can be assigned to a phenyl ring bending predicted at 1403 cm^{-1}, a mode scarcely affected by the environment. Probably the surrounding structure originates from an overlap between this signal and a weak one relative to a broader δ_{ll}(H-bond) normal mode of the acid dimer, which is known to fall in this region.

(21) This peak is a shoulder of the band detected at 1577 cm^{-1}.

(22) As one example, we have found another relative minimum, higher in energy by 12.75 kcal/mol, for the $L1Na_2$ *syn* conformation where the planes of the carboxylate moieties are rotated around the $C-CH_2$ bond about 90° with respect to the most stable geometry. Force calculations on this geometry give for the $\nu_{as}^{+}(COO^-)$ normal mode a frequency of 1583 cm^{-1} and an intensity of 323 KM/mol, while for the $\nu_{as}^{-}(COO^-)$ one a frequency of 1568 cm^{-1} and an intensity of 423 KM/mol are obtained. Despite the decreased agreement with the experimental frequency data, this proves that a small variation of the carboxylate orientations can destroy the C_2 symmetry of the molecule and consequently increase the intensity of the band associated to the $\nu_{as}^{-}(COO^-)$ mode, which for a true C_2 symmetry would have an exactly zero intensity.

(23) NICODOM IR Organics and Inorganics infrared spectra library, www.ir-spectra.com.

JP807203N